Workshop on Virtual Reality Interaction and Physical Simulation VRIPHYS (2015)
F. Jaillet, G. Zachmann, and F. Zara (Editors)

Vascular neurosurgery simulation with bimanual haptic feedback

J. Dequidt[1] & E. Coevoet[2] & L. Thines[3] & C. Duriez[2]

[1]University of Lille, France
[2]Inria, France
[3]Hospital of Besancon, France

Abstract

Virtual surgical simulators face many computational challenges: they need to provide biophysical accuracy, realistic feed-backs and high-rate responses. Better biophysical accuracy and more realistic feed-backs (be they visual, haptic...) induce more computational footprint. State-of-the-art approaches use high-performance hardware or find an acceptable trade-off between performance and accuracy to deliver interactive yet pedagogically relevant simulators. In this paper, we propose an interactive vascular neurosurgery simulator that provides bi-manual interaction with haptic feedback. The simulator is an original combination of states-of-the-art techniques that allows visual realism, bio-physical realism, complex interactions with the anatomical structures and the instruments and haptic feedback. Training exercises are also proposed to learn and to perform the different steps of intracranial aneurysm surgery (IAS). We assess the performance of our simulator with quantitative performance benchmarks and qualitative assessments of junior and senior clinicians.

Categories and Subject Descriptors (according to ACM CCS): I.3.8 [Computer Graphics]: Computer Graphics—Applications I.3.7 [Computer Graphics]: Computer Graphics/Three-Dimensional Graphics and Realism—Virtual reality

1. Introduction

Training in cerebrovascular surgery, and particularly Intracranial Aneurysm Surgery (*IAS*), is a concern of many neurosurgery residency programs all over the world due to the drastic reduction in operated cases following the development of endovascular procedures those past twenty years. Indeed, because of the drop in operated cases due to the strong development of interventional neuroradiology since the ISAT and ISUIA studies [MG*02, WoUIAI*03], the training of residents and fellows in those neurosurgical procedures became difficult, and this is particularly true in France where 60 up to 90% of cerebral aneurysms are nowadays treated by endovascular means [LPJ12]. Comparable figures are found in most western countries. This situation is in total contradiction with the high level of expertise that is required regarding the life threatening, urgent and complex nature of ruptured intracranial aneurysms and that is expected by the patients and the healthcare system itself.

Simulation-based Virtual Reality (*VR*) applications have reached the medical community through the development of training simulators that allow the acquisition of skills and gestures in a reproducible, controlled, supervised and ethical environment. Such simulators allow to increase the available training time for residents or experienced clinicians since several studies exhibit a positive correlation between experience / training time and patient outcome [CDP07, BWR*09]. However, despite several governmental incentives [GC04] few clinical curricula require training on simulators. De Visser *et. al.* [DVWS*11] report that while the benefits of VR simulators are indisputable to train novice-to-intermediate skills, they are yet not suitable for the training and maintenance of advanced skills. Insufficient level of physical realism, incomplete performance assessment and modest case complexity are suggested by De Visser *et. al.* to be the main limitations to use simulators for surgical curricula. From a computer graphics standpoint, these criteria can be elaborated as:

- *Visual Realism*: organs or anatomical structures are ge-

DOI: 10.2312/vriphys.20151337

ometrically complex objects and should be described as precisely as possible while having a reasonable number of primitives (triangles for instance) to be rendered interactively. Textures are also an important concern since the overall aspect of an organ provides lots of relevant information to clinicians (wealthy vs ill tissue, sufficient level of moisture...). Therefore having realistic textures is an important feature to have in a VR simulator.

- *Physical Realism*: the behavior of anatomical structures should mimic the motion and deformation of actual structures during surgery. This induces the need for accurate bio-physical models, characterized using patient data but also requires to be able to handle complex interactions between structures or between anatomical structure and surgical devices such as grasping, friction, sliding...
- *Haptic Feedback*: relevant training involves to perform the same manipulation in the simulators and in an actual procedures. Clinicians heavily rely on touch to assess the softness / rigidity of tissue and to prevent complications to happen. As a consequence, the haptic feedback should be accurate and be delivered at a sufficient rate. In the case of IAS procedures, clinician use their both hands to do the surgery: one is used to give access to the aneurysm by pushing brain tissues while the other perform the surgery (cutting, clipping...). The simulator should be able to manage bi-manual accurate haptic feedback.

We will shortly shortly describe a standard IAS procedure in order to detail what the simulator should provide, some steps of the procedure are also illustrated on figure 1:

- *General set-up*: binoculars are set to provide visual feedbacks to the aneurysm, the surrounding arteries and brain tissues. Clinician will use both hands and several surgical devices to perform the procedure:
- *Open craniotomy*: Under general anesthesia, an opening is made in the skull exposing a part of the brain.
- *Sylvian fissure dissection*: the main idea is to separate two lobes of the brain which gives access to the aneurysm. Once separated, the lobes are gently moved to provide a working area around the aneurysm.
- *Aneurysm clipping*: the aneurysm is then clipped on the aneurysm. This is the most complex step: the working area is really tight and manipulation around the aneurysm must not touch heavily the aneurysm in order to prevent aneurysm rupture. In case of aneurysm rupture, blood will fill the working area and removes all visibility. And the surgeon will have to clean the working space with a small blood sucker (and he will also have to clip faster in order to limit the blood loss). Special care is also taken not to clip a parenting artery which could lead to important damages for the patient.

Contributions The motivation of this paper aims at addressing most of these issues. More specifically we would like to provide a virtual reality simulator that includes visual realism of the anatomical structures (except the textures

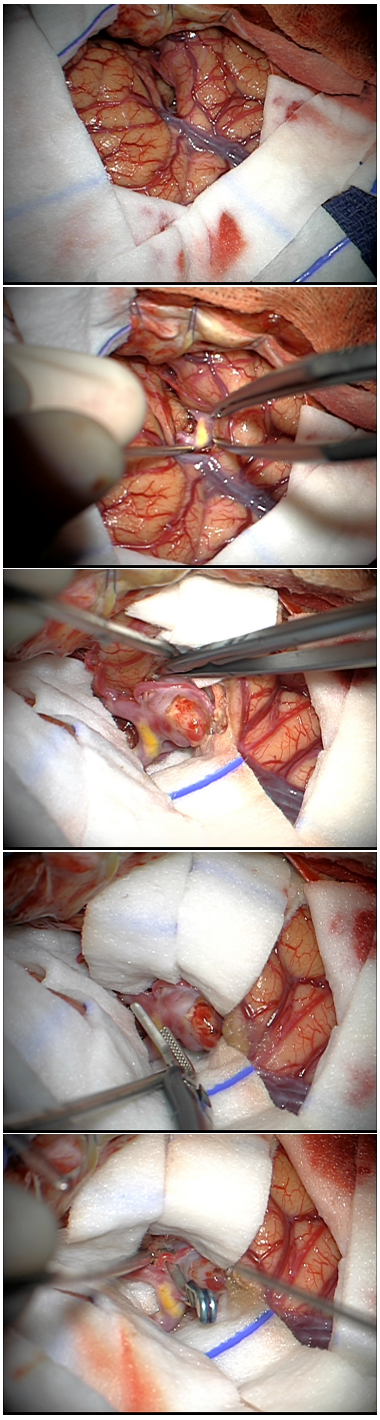

Figure 1: *Several steps of an IAS procedure: first a craniotomy is performed; second the sylvian fissure is dissected to separate brain lobes; third the aneurysm is exposed; fourth a clip is set on the aneurysm; fifth the clip is in place.*

which requires contributions in a completely different domain), physical realism of the brain and the vascular tree and their interactions with surgical devices and high quality haptic feedback. All these features should be integrated in a single environment and should run at interactive rates. Moreover several exercises will be proposed to train specific steps of the procedure. Compared to recent works such as [FD15] and [ALB*15], we handle the connective tissues that link the brain tissues and we also propose an asynchronous method that provides high-speed haptic feedback even for complex FEM simulations.

In this paper, we demonstrate the feasibility of a realistic training for vascular neurosurgery procedure using virtual reality systems. The contribution of the paper is not a novel algorithm or a numerical method but rather an original combination of state-of-the-art algorithms and models that allows to obtain this first demonstrator of bi-manual haptic virtual reality simulation for training in intracranial aneurysm surgery.

2. Previous Work

Brain tissue deformation models There are several motivations which have led to researches on mechanical simulations of brain tissues:

- Brain shift (e.g. hydrocephalus) during surgery: The loss of cerebro-spinal fluid creates a global deformation (a shift) which changes the configuration of the brain. The goal of the researches is to obtain an intra-operative registration so that the surgeon can more easily locate important structures of the brain during the surgery. In such case, the simulation is driven by images [MPH*00].
- Behavior in case of extreme mechanical load (a car crash for instance). The simulation aim at predicting the resulting damages on the tissues [Bil11].
- Training simulation which requires real-time and realistic behavior, but not necessary predictive simulations. In this category, which is more in the focus of our work, we find the work of [EHA*14], based on a hyperelastic model with explicit integration and [PMRA09] which relies on mass-spring method.

Between the related papers, there is an important variation of values when it comes to type of constitutive laws and the parameter estimation of the deformable models. According to [Bil11], *"it is unrealistic to expect that one constitutive model will fit all circumstances"*. Indeed, the brain model should be selected according to the application.

Haptic rendering of soft tissues Haptic rendering enables a physical interaction with simulated objects of a virtual environment. Somehow, it provides a ground truth on the accuracy of the physics-based models used in an interactive simulation. However, the link between the quality of haptic feedback and the accuracy of the interactive simulation is not direct. Indeed, as the real-time constraints of haptic feedback are even more severe, it is difficult to maintain the same level of quality in the modeling, especially in the context of soft tissues. Several approaches have been proposed to deal with the constraints imposed by haptic rendering: high frequency refresh rates, stability of the control, fidelity perceived by the user.

A first approach is the use of an explicit integration scheme for the deformable model (FEM, Mass-springs or other models) [ZC99] [FLA*05] [PL99]. The explicit integration allows for fast computations at each time step (only the mass matrix, which can be lumped as a diagonal matrix is involved) but the methods are often difficult to stabilize and the rendering is only possible on very soft objects.

An other direction of research is the use of pre-computations. In the pioneering works [CDA99], a linear FEM deformable model is pre-computed and pre-condensed on the mesh points of the surface. When a collision accurs with an haptic probe, a system of equality constraints is solved by a method of Lagrange multipliers. The method is extended in [MH04] and [PSBM10] to more complex deformable models. Stable haptic rendering is achieved, since the response forces are efficiently calculated from *precomputed data*, e.g. by interpolation, performed directly in the haptic loop. In [JP05], a unified approach to the interaction with elasto-static contact simulation is presented. In this case, the contact resolution is based on a *capacitance matrix* which relates the imposed displacements and response forces. Although viscoelastic and non-linear models are employed, only point-based interaction is considered due to limitations given by the pre-computations.

In [BJ08], the contact problem is solved using a *penalty-based method* allowing for multiple contacts and self-collisions. Both tool and obstacle are deformable and simulated by finite elements methods optimized thanks to model reduction. However, the penalty-based methods cannot guarantee the non-interpenetration, they are very sensitive to the choice of the penalty parameters and do not integrate properly static/dynamic friction. In the context of haptic rendering, it could lead to additional problems with stability.

Based on an example of virtual snap-in simulations [DAK] introduced Signorini's model for contact handling in the context of haptic rendering of deformable objects. The approach is extended to rendering of dry and dynamic friction in [DDKA06] with the formulation of a NLCP (non-linear complementarity problem) but is limited to small linear deformations. To extend to non-linear deformable tissues, a simplified representation of the simulation is often employed for the haptic loop, like the diagonal blocks of the (N)LCP matrix in [GO09]. In [CADC11], the combination of GPU computation and the use of an asynchronous computation of a pre-conditioner allows to greatly improve the precision while keeping fast computations in the simulation (50 frames/sec). In [PND*11] the NLCP computed in the

simulation is shared with the haptic loop and re-solved at high rates.

In this paper, we combine the two previously mentioned methods for allowing haptic rendering of the non-linear FEM model of the brain when they are in contact or in interaction with the instruments (clips, graspers).

3. 3D modeling of the virtual surgical scene

3.1. Geometric Modeling

As mentioned in the introduction, the virtual surgical scene should be faithfully reproduced in the virtual environment and more specifically the anatomy. Therefore we choose to acquire the anatomy through anonymous patient. Specific 3D imaging data of a patient carrying a right unruptured middle cerebral artery (MCA) aneurysm were acquired as part of the routine preoperative work-up and transferred as a DICOM. A manual segmentation of the 4 main structures of interest (cranial bone, cerebral hemisphere, intracranial arteries and MCA aneurysm) was performed by a surgical expert. Native images of the cranial bone and cerebral arteries were obtained from a preoperative 3D-CTA scan with iodine contrast injection. The 3D reconstruction of the bone structures was performed using a simple thresholding segmentation method [FM81]. The fashioning of the desired craniotomy (drilling of the skull) was performed manually using the cutting tool in the software and was designed to offer a wide exposure of the sylvian fissure and of the middle cerebral artery tree. For this simulator, we choose not to train for the craniotomy since this step does not require specific expertise and therefore our skull model has been drilled during the segmentation. The volumes of the parasylvian areas, frontal and temporal edges, were meshed separately with tetrahedrons using the open-source Computational Geometry Algorithms Library (CGAL) (figure 2 bottom).

Native images of the brain parenchyma and of the arteries/aneurysm were obtained using a preoperative 3D-MRA scan of the brain with contrast enhancement on a 1.5 T MRI scanner (Achieva, Philips Medical Systems, Best, Netherlands). The 3D reconstruction of the volumes of the temporal lobe, the remaining hemisphere and the arteries/aneurysm were performed separately and semi-automatically to allow individualized biomechanical simulation (figure 2 top).

Basic surgical tools (suction tool, micro-stylus dissecting tool and brain retractors) were designed using a 3D modeling software. A common set of miniature and standard aneurysm clips (B. Braun-Aesculap, Tuttlingen, Germany) and their applier were digitized using the same 3D-CT scanner and were segmented using ITK-SNAP (figure 2 top).

3.2. Surgical Complications

Aneurysm rupture is simulated by the adjunction of a trigger zone on an aneurysmal bleb when accidental collision

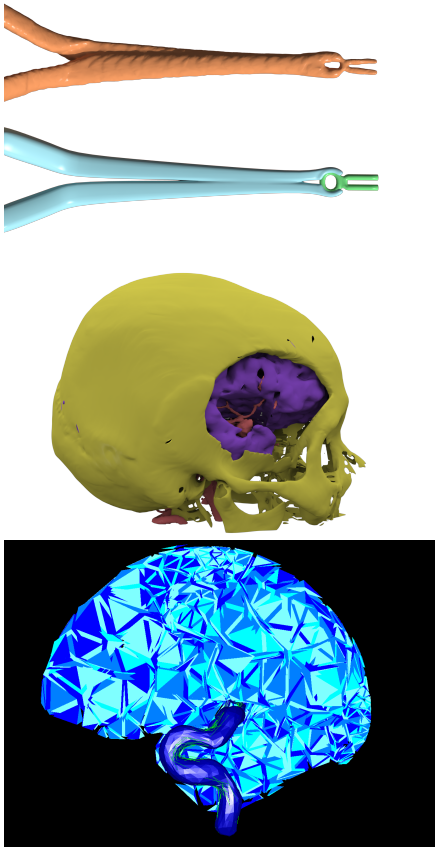

Figure 2: *3D modeling of the surgical scene: (top) segmented clip and applier in orange and the meshes used for the simulator in blue and green (middle) the geometric model of the skull (yellow), cerebral hemisphere (purple) and arteries (red); (bottom) tetrahedral mesh of the brain hemisphere*

when a surgical device occurs. The bleeding is simulated as a clipping plane that fills the operative field. A suction tool is available to reduce the blood level and a temporary clip can be placed on the vessel that supplies the blood in the ruptured aneurysm. From a programming standpoint, the level of bleeding is then regulated backward and forward by the contact between the tip of the suction tool and this plan. The bleeding can be stopped by the application of a temporary clip on the vessel that supplies the blood in the ruptured aneurysm. It is worth mentioning that this complication can be very harmful for the patient and the temporary clip should be removed and the final clip should be definitely placed five minutes after the bleeding has started. In the simulator, when an aneurysm is ruptured a counter is triggered and displayed on screen to indicate the remaining time to place the final clip (see figure 6 bottom).

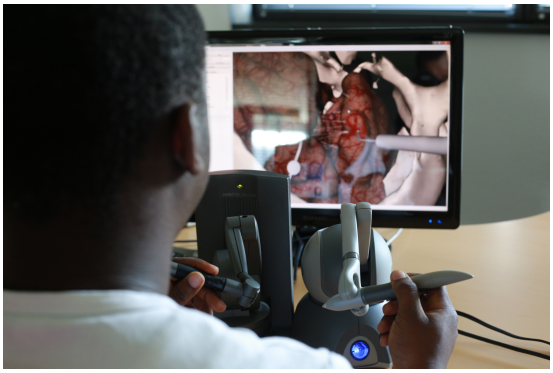

Figure 3: *Photography of the set-up where a trainee uses two haptic arms to interact on the surgical physical simulation.*

3.3. Hardware set-up

The simulator consists in a double haptic force feedback virtual reality application. Visualization of the surgical scene was presented in this initial prototype in a non-stereoscopic 3D environment and on a 2D flat screen, which made the evaluation of the depth and the progression of the instruments in the operative corridor sometimes a bit uncertain. In order to solve this problem, we have tested the adjunction of a virtual reality head-mounted display (i.e: Oculus Rift, Oculus VR). Nevertheless, this modification was accompanied by a decrease in image definition, which precluded its regular use at this stage of development. The forces feedback was rendered to the operator using two haptic arms (Phantom Omni, Sensable) and some scripts were developed in Python to allow tools exchange (a picture of the set-up is available on figure 3).

4. Real-time bio-mechanical models

To reproduce a realistic behavior of the tissues during the simulation, we have proposed physics based models for brain tissues, vessel walls and arachnoidal strands, described in this section. The dynamics of the model is computed using an implicit integration.

4.1. Time stepping implicit integration

Let's consider a generic dynamic deformable model. Equations used to model the dynamic behavior of bodies is given by the Newton's second law:

$$\mathbf{M}\ddot{\mathbf{q}} = \mathbf{f}^{\text{ext}} - \mathbf{f}^{\text{int}}(\mathbf{q},\dot{\mathbf{q}}) + \mathbf{H}^{\text{T}}\lambda \qquad (1)$$

where $\mathbf{q} \in \mathbb{R}^n$ is the vector of generalized degrees of freedom, $\mathbf{M}$ is a mass (intertia) matrix, $\mathbf{f}^{\text{ext}}$ and $\mathbf{f}^{\text{int}}$ are respectively the vectors of the external and internal force. $\mathbf{H}^{\text{T}}\lambda$ gathers the constraint forces contributions.

To integrate these equations over time, we chose to use implicit Euler integration scheme with a constant time step h.

$$\dot{\mathbf{q}}_{t+h} = \dot{\mathbf{q}}_t + h\ddot{\mathbf{q}}_{t+h}$$
$$\mathbf{q}_{t+h} = \mathbf{q}_t + h\dot{\mathbf{q}}_{t+h}$$

We also apply a single linearization of the internal forces by time step using a Taylor series extension

$$\mathbf{f}^{\text{int}}(\mathbf{q}_{t+h},\dot{\mathbf{q}}_{t+h}) \approx \mathbf{f}^{\text{int}}(\mathbf{q}_t,\dot{\mathbf{q}}_t) + \frac{\partial \mathbf{f}^{\text{int}}}{\partial \mathbf{q}}\mathrm{d}\mathbf{q} + \frac{\partial \mathbf{f}^{\text{int}}}{\partial \dot{\mathbf{q}}}\mathrm{d}\dot{\mathbf{q}} \qquad (2)$$

Using $\mathrm{d}\mathbf{q} = \mathbf{q}_{t+h} - \mathbf{q}_t$ and $\mathrm{d}\dot{\mathbf{q}} = \dot{\mathbf{q}}_{t+h} - \dot{\mathbf{q}}_t$, we finally obtain a linear system of equation:

$$\begin{aligned} &\mathbf{A}\,\mathrm{d}\mathbf{q} = \mathbf{b} \\ &with: \\ &\mathbf{A} = \left(\frac{\mathbf{M}}{h^2} + \frac{\partial \mathbf{f}^{\text{int}}}{\partial \dot{\mathbf{q}}}\frac{1}{h} + \frac{\partial \mathbf{f}^{\text{int}}}{\partial \mathbf{q}}\right) \\ &\mathbf{b} = \mathbf{f}^{\text{ext}} - \mathbf{f}^{\text{int}}(\mathbf{q}_t,\dot{\mathbf{q}}_t) + \left(\frac{\mathbf{M}}{h} - \frac{\partial \mathbf{f}^{\text{int}}}{\partial \dot{\mathbf{q}}}\right)\dot{\mathbf{q}}_t + \mathbf{H}^{\text{T}}\lambda \end{aligned} \qquad (3)$$

This system is solved for every deformable model at every time step. To solve the system, we employ a conjugate gradient algorithm combined with a preconditionner computed on GPU, like described in [CADC11].

4.2. Brain Model

During the surgery, the deformation of the brain essentially comes from the mechanical interaction with the instruments. An other source of deformation is the leak of Cerebro-Spinal Fluid (*CSF*), but we have chosen to ignore this phenomenon which is very slow and not critical in a context of training. We made a trade-off between real-time performance and precision by selecting a FEM model, based on corotational approach (linear elastic constitutive law but the model account for large displacements). For the parameters of the model are the Young Modulus $E = 2100$Pa and Poisson Coefficient $\nu = 0.45$, which corresponds to data given in [MPH*00]. The mass density is set to $1g/cm^3$.

We use two separate meshes for the two lobes of the brain that are separated during the sylvian fissure dissection (see section 3.1 for geometrical modeling). The front lobe is composed of 550 nodes and 1556 elements and the temporal lobe of 330 nodes and 946 elements.

4.3. Vessel Model

The apparent rigidity of the vessels when touched by surgical instruments comes from the natural resistance to deformation of the vessel wall combined with the pressure induced by the blood. During real intervention, it is sometimes possible to observe the pulsatility of the blood flow. For modeling the vessels, we combine a FEM model of the surface of the vessel, based on membrane modeling [CDC10] combined with a pressure constraint. This pressure constraint simply applies a constant pressure on the vessel walls.

In the model, $\mathbf{H}^{\mathrm{T}}$ represents a vector which contains the normal vector at the points of the vessel mesh, weighted by the areas of the neighboring triangles. λ represents a pressure that we can tune manually.

The value of $\mathbf{f}^{\mathrm{int}}(\mathbf{q},\dot{\mathbf{q}})$ is given by FEM membrane model (note that the damping relies on Rayleigh model). For each point, we assign a small mass value in a diagonal matrix $\mathbf{M}$. To improve the stability of the model, we also add bending springs (i.e. springs that prevents the bending deformations) and soft linear springs (each point is compliant but somehow *attached* to its initial position). As we can not simulate all the existing connections between the brain and the vessels, we use this simplified approach to model the environment and the boundary conditions of the vessel model.

4.4. Arachnoidal strands

These connective tissues have a very important role from a mechanical point of view because they *stick* the brain lobes together. During the dissection of the Sylvian fissure, these strands are being cut by the surgeons in order to access the aneurysm. Moreover, in the final access to the aneurysm, the surgeon should also remove the strands that link the brain tissues to the vessels. This is a delicate gesture, the instrument should ideally cut the strands without damage on the surface of the brain lobes or on the vessel walls.

These strands are composed of elastic tissue which is difficult to characterize precisely. But more than a constitutive model, we think that the model should provide adequate boundary conditions on the anatomical structures that are linked by these strands and cutting force on the instruments that cut the strands.

Consequently, for the constitutive model, we use a simple spring that links two points that belongs to the brain lobe models and/or to the vessel model, depending on the case. The strands are visible in the two first pictures of Figure 6. We emphasize that the two points could be placed on two deformable models that are, somehow, independent (not the same mesh, not the same solver). Thus, to create an adequate behavior, we model this spring as a constraint:

$$\lambda = k(\|\mathbf{q}_i - \mathbf{q}_j\| - l_0)$$

where k is the stiffness coefficient of the strand model, l_0 is the initial lenght, and $\mathbf{q}_i$ $\mathbf{q}_j$ are points at the extremity of the strand, this points can be either nodes of the brain models or of the aneurysm model. The direction of the spring force is put in the $\mathbf{H}$ matrix. For instance, for point i:

$$\mathbf{H}_i^T = \frac{\mathbf{q}_i - \mathbf{q}_j}{\|\mathbf{q}_i - \mathbf{q}_j\|}$$

Thus, the strands are been solved as a special case of bilateral constraints.

Each strand can be be cut by the blade of a surgical instrument. To simulate the resistance to cutting, when a collision is detected between the strand and the blade, we do not directly remove the strand. We simulate a contact that progressively reduces k till it reaches zero. When $k = 0$, we remove the strand.

5. Bimanual constraint-based haptic rendering

This section describes the models and algorithms that are employed for the simulation of the interactions of the neurosurgical instruments with the brain tissues and the corresponding haptic rendering. As stated in section 2, we combine the methods of [CAK*14] and [PDC11] while extending to bi-manual haptic feedback and integrating new type of constraints like the ones developed for arachnoidal strands.

First, we do a projection of the mechanical models in the constraint space. Let's consider a mapping function $\mathcal{M}(\mathbf{q})$ which provides the violation δ of the constraint given the position $\mathbf{q} = \mathcal{M}(\mathbf{q})$ of the degrees of freedom of the system. We linearize the computation of this violation in the neighbourhood of its value when $\lambda = 0$ (i.e. during a free motion $\delta^{\mathrm{free}} = \mathcal{M}(\mathbf{q}^{\mathrm{free}})$ with $\mathbf{q}^{\mathrm{free}}$ solution of equation (1) when $\lambda = 0$.).

$$\delta = \mathcal{M}(\mathbf{q}) \approx \underbrace{\frac{\partial \mathcal{M}}{\partial \mathbf{q}}(\mathbf{q})}_{\mathbf{H}} \mathrm{d}\mathbf{q} + \delta^{\mathrm{free}} \tag{4}$$

Then, we integrate equation 3 and compute the Schur complement:

$$\delta = \mathbf{H}\mathbf{A}^{-1}\mathbf{H}^T + \delta^{\mathrm{free}} \tag{5}$$

In the following $\mathbf{W} = \mathbf{H}\mathbf{A}^{-1}\mathbf{H}^T$. Finally, the Lagrange multipliers values are computed by a mixed non-linear complementarity problem solver:

$$\begin{aligned}
&\delta = \mathbf{W}\lambda + \delta^{\mathrm{free}} \\
&0 = \delta_i && \text{(bilateral)} \\
&0 \le \delta_j \perp \lambda_j \ge 0 && \text{(contact)} \\
&\|\lambda_k\| \le \mu\lambda_k \;\&\; \dot{\delta_k} = 0 \perp \|\lambda_k\| = -\mu\lambda_j \frac{\dot{\delta_k}}{\|\dot{\delta_k}\|} && \text{(friction)}
\end{aligned} \tag{6}$$

where constraints i gathers all the bilateral constraints, constraints j correspond to Signorini's contact and constrains to Coulomb's friction.

The problem is solved using a Gauss-Seidel like iterative solver, which solves the constraints block by block (for instance contact and friction constraints on the same contact point are solved together in a block, see [DDKA06] and [PDC11] for details). In [PDC11], it is highlighted that building the system (and especially computing matrix $\mathbf{W}$) is consuming more time than solving the system, especially if a *warm start* value λ_0 is provided at the fist iteration of the Gauss-Seidel.

Multithreading with bimanual haptic rendering : In [PDC11], this observation leads to a multi-threading approach where the system described by equation (6) is shared

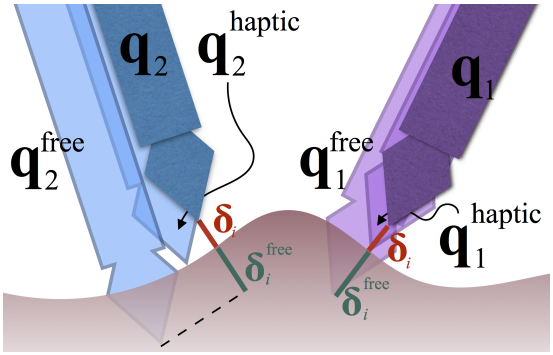

Figure 4: *Several positions are computed for each instruments:* $\mathbf{q}_1$ *and* $\mathbf{q}_2$ *are the positions in the simulation and* $\mathbf{q}_1^{\text{haptic}}$ *and* $\mathbf{q}_2^{\text{haptic}}$ *the positions in the haptic loop. The free positions* $\mathbf{q}_1^{\text{free}}$ *and* $\mathbf{q}_2^{\text{free}}$ *are updated in the haptic loop thanks to the measure at high rate of the device motion*

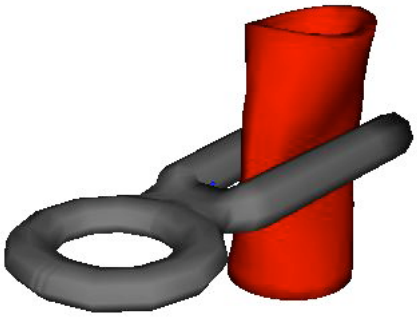

Figure 5: *Illustration of vessel clipping using contact and friction constraints*

between the simulation and a haptic loop. In the simulation the system is build and and solved, then, it is shared with the haptic feedback and re-solved at high rates.

The temporal coherency of the deformable models associated with a predictive collision detection (we compute the minimal distances between meshes) make the (in-)equations change only little from one step to an other in the simulation. Yet, the results of the solver could change a lot, particularly when a contact occurs (δ_j^{free} becomes negative and λ_j which was zero before contact becomes strictly positive). This is very important to capture this changes at high rates in the haptic loop for the transparency of the rendering.

The principle of the method is simple: it updates the value of δ^{free} given the position changes of the haptic device and re-solve, at high rates, the value of λ in the system. For this simulator, we have extended the approach to two haptic devices while keeping a coherent haptic rendering.

For a bimanual haptic feedback, two rigid instruments are simulated and interacts with the deformable models. Let's suppose that vector $\mathbf{q}$ is composed of three vectors $\mathbf{q}_1$, $\mathbf{q}_2$ and $\mathbf{q}_3$. $\mathbf{q}_1$ represents the 6DoFs position of the first instrument (in practice a vector of size 3 for the translation and a quaternion for the orientation) and $\mathbf{q}_2$ the position of the second instrument. $\mathbf{q}_3$ gathers all the degrees of freedom of the deformable models.

The free position of the instruments $\mathbf{q}_1^{\text{free}}$ and $\mathbf{q}_2^{\text{free}}$ is given by the position of the two devices (see figure4). Between this position and the actual position (in both simulation and haptic loop), we simulate a 6DOF spring. Let's suppose that we have set the non-linear complementarity problem at time T in the simulation. We can update the value of δ^{free} when new information is coming from the position sensors of the device at time $T + dT$:

$$\delta_{T+dT}^{\text{free}} = \delta_T^{\text{free}} + \mathbf{H}(\mathbf{q}_1)(\mathbf{q}_{1,T+dT}^{\text{free}} - \mathbf{q}_{1,T}^{\text{free}}) + \mathbf{H}(\mathbf{q}_2)(\mathbf{q}_{2,T+dT}^{\text{free}} - \mathbf{q}_{2,T}^{\text{free}}) \quad (7)$$

This update of δ^{free} can be performed very quickly and given the result, we can start a set of iterations of the Gauss-Seidel (GS) algorithm in the haptic loop. In practice, the GS iterates during $1ms$ without testing any convergence criterion to have the best possible values in the haptic loop.

We emphasize that, with this method, the haptic feedback for the two device is a result of a unique mixed non-linear complementarity problem. Consequently, the coupling between the instruments and eventually the rendering of their collision is naturally taken into account. The precision of the contact and friction model allow for complex interactions. In the case of a vascular neurosurgery simulation, vessel clipping is particularly challenging (the clip must remain around the vessel) as illustrated in Figure 5.

6. Results

This section presents the scenarios that are available on the simulators and discuss both technical performance and preliminary evaluation.

Pedagogic scenarios For the sake of this simulation procedure, the surgical scene was represented after craniotomy (opening of the skull). Four pedagogic scenarios representing the different steps of the approach and of the final clipping were proposed. Force feedback is transmitted to the operator by two haptic arms at every step of the procedure.

- In scenario 1, the operator has to perform the sylvian fissure opening by gently retracting the frontal or temporal lobe of the brain with the suction tool in his left hand and cutting the arachnoidal strands from the surface to the depth with the dissecting tool in his right hand.

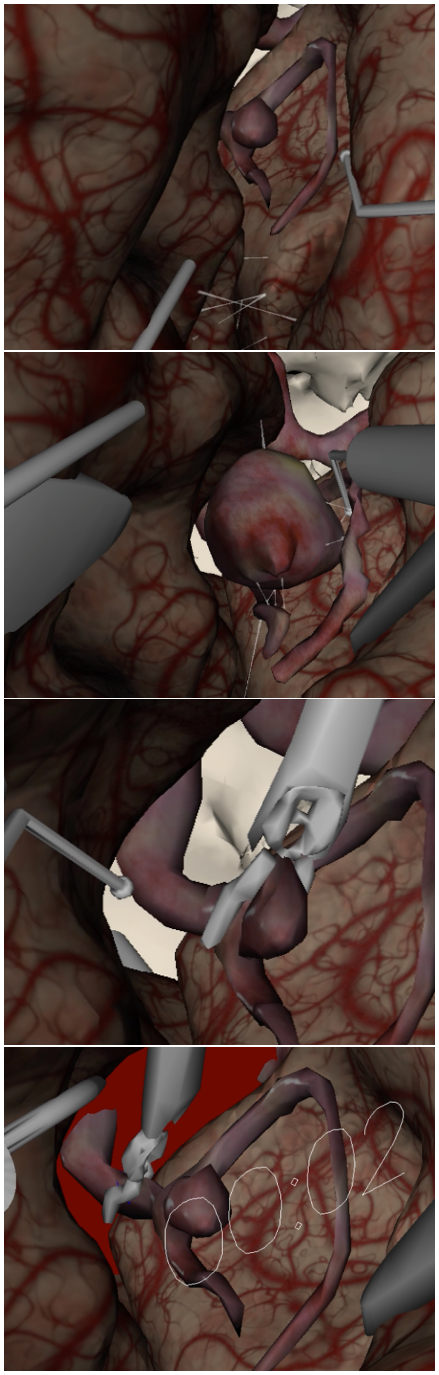

Figure 6: *Simulation steps: Sylvian fissure opening, Aneurysm dissection, Aneurysm Clipping, temporal clipping in case of bleeding*

- In scenario 2, the sylvian fissure is widely split and, for the sake of the simulation, is maintained opened by frontal and temporal brain retractors. Hence, the operator can concentrate on the aneurysm dissection by progressively removing with the tip of the micro-stylus the arachnoidal strands placed between the sac and the cortical surface or adjacent arterial branches of the bifurcation. Bi-manual work involves retracting the brain or the arteries with the suction tool in one hand and dissecting the arachnoid with the micro-stylus in the other hand. The exercise stops when all the arachnoidal strands are divided.
- In scenario 3, the operator has to select the appropriate clip in a library of 8 digitized clips displayed on a drop-down menu. The clip is initially placed on the applier (instrument that deliver the clip). It could be released or retrieved easily in the operative field at any time by pressing a button on a stylus of the haptic device. The widening or tightening of the clip is controlled by the other button. The collision detection and response creates the deformations of the aneurysm wall under clip jaw forces. The goal of the exercise is to have a good tightening of the aneurysm neck without any obstruction on other collateral arteries. If necessary, the observer can challenge the trainee by asking him to remove the clip and to position it properly.
- In scenario 4, the trigger zone for *rupture* is activated on the aneurysm wall. When the operator touches it involuntary (or by the supervisor's command), a bleeding occurs and forces him to quickly react. The level of blood in the operative field could be controlled by the use of the suction tool in one hand followed by the application of a temporary clip on the connecting artery with the applier in the other hand. We emphasize that the blood physics is not simulated and that the level elevation is reproduced only visually. When the temporary clip is delivered, a timer displays automatically on the screen. A limited amount of time (i.e.: 3 minutes) could be allocated to the user in order to clip the aneurysm and then remove the temporary clip.

Technical performances and limitations The average performance obtained in the simulation is around 30 frames per second (fps).When the clip is closed at the aneurysm neck, this framerate decreased around 25 fps (for 40 contact points detected with friction so 120 constraints). This change in the performance does not impact the normal assessment of the quality of clipping by rotating the surgical scene. The reader may refer to figure 7 where detailed benchmarks are available and exhibit a steady frame-rate (simulation time) even with a high number of constraints.

Bi-manual coordination, surgical strategy, reactivity, stress management and quality of clip application could be assessed in real time due to the optimization of the computational time.

Limitations:

- The computation of the matrix **W** for the blood vessels

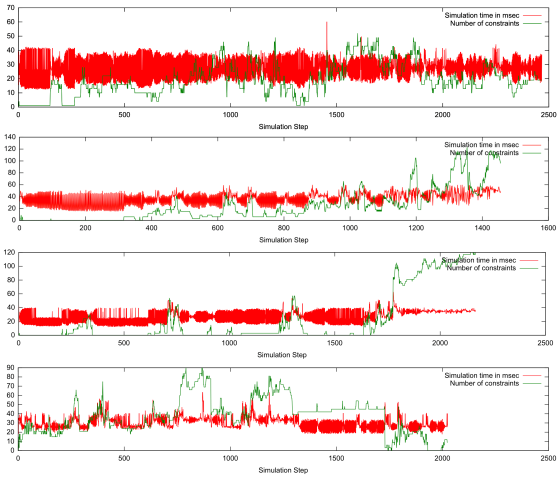

Figure 7: *Performance benchmarks: for each exercise (4 total), we plot the time require to compute the simulation and the number of constraints. The number of constraints does not significantly increase the simulation step which remains interactive throughout the exercises.*

Question / Response	Yes	Yes	p values
Appropriateness of scenarios	16	14	0.34
Visual quality	13	13	0.46
Realism of interactions	10	8	1
Realism of haptic rendering	6	3	1

Table 1: *Summary of the feedbacks reported by neurosurgeons (NS). 17 junior NS and 14 senior NS were involved in this qualitative evaluation.*

is simplified which reduces the haptic realism when the tools are in contact with the vessels.

- After the release of the clip, it is no more simulated (fixed in space): It allows to reduce the complexity and avoid motion of the clip. In real case, the clip is maintained by surrounding tissues that are not present and represented in our scenario. This would greatly increase the number of contact and the complexity of the scene.

Evaluation Thirty-one operators (17 junior neurosurgeons and 14 senior neurosurgeons) practiced on the prototype and gave their opinion. The vast majority of the users (97%) were convinced that this tool would be helpful in the future for training in IAS. All the operators (100%) managed to manipulate the different tools, to divide the arachnoid strands and to clip the aneurysm. The feedback analysis (see table 6) revealed that the selection of the surgical scenarios, the visual quality of the surgical scene, the realism of bi-manual manipulations and of the haptic force feedback rendering were found appropriate respectively by 97%, 84%, 58% and 29% of the users. No significant statistical differences were found between the evaluations of junior and senior NS ($p > 0.05$). The most frequent recommendations expressed by the users were: the implementation of a 3D stereoscopic visualization to introduce depth perception, the redesigning of the surgical instruments aspects, the improvement of the haptic force feedback realism (resistance of brain parenchyma, pulsatility of the vessels), and the development of different types of aneurysm (simple or complex).

7. Conclusion and Future Work

The technical design of this prototype allows representing the approach and clipping of intracranial aneurysms with realistic, real-time, interactive and bi-manual haptic rendering. We have also proposed with this simulator the most complex and detailed virtual training program for intracranial aneurysm surgery to date. If many improvements are still needed to get closer as possible to reality, our simulator certainly opens the way for the development of more sophisticated platforms of simulation of cerebrovascular surgery. More specifically, some approximations or simplifications are made in our simulator that need to be addressed in a near future. For instance, the compliance matrix of the blood vessels is simplified and the surrounding brain tissues that prevent the clip from moving are not present. The overall realism of the simulator can be improved by having more accurate or detailed bio-mechanical models of the anatomical structures but the main challenge is to conserve an interactive rate for the computation. To do so, GPGPU approaches or Proper Orthogonal Decomposition (POD) will be investigated. From a pedagogic viewpoint, more complications should be added in the simulator and should be randomly triggered during exercises in order to assess the behavior of surgeons under stress and unexpected events. Finally, quantitative metrics should be defined and recorded in order to provide the surgeons detailed performance feed-backs about the exercises they have completed.

References

[ALB*15] ALARAJ A., LUCIANO C. J., BAILEY D. P., ELSENOUSI A., ROITBERG B. Z., BERNARDO A., BANERJEE P. P., CHARBEL F. T.: Virtual reality cerebral aneurysm clipping simulation with real-time haptic feedback. *Operative Neurosurgery 11*, 1 (2015), 52–58. 3

[Bil11] BILSTON L. E.: Brain tissue mechanical properties. In *Biomechanics of the brain*. Springer, 2011, pp. 69–89. 3

[BJ08] BARBIČ J., JAMES D. L.: Six-dof haptic rendering of contact between geometrically complex reduced deformable models. *IEEE Trans. Haptics 1*, 1 (2008), 39–52. 3

[BWR*09] BOUDOURAKIS L. D., WANG T. S., ROMAN S. A., DESAI R., SOSA J. A.: Evolution of the surgeon-volume, patient-outcome relationship. *Annals of Surgery 250*, 1 (2009), 159–165. 1

[CADC11] COURTECUISSE H., ALLARD J., DURIEZ C., COTIN S.: Preconditioner-based contact response and application to

cataract surgery. In *Medical Image Computing and Computer-Assisted Intervention (MICCAI)* (2011). 3, 5

[CAK*14] COURTECUISSE H., ALLARD J., KERFRIDEN P., BORDAS S. P., COTIN S., DURIEZ C.: Real-time simulation of contact and cutting of heterogeneous soft-tissues. *Medical image analysis 18*, 2 (2014), 394–410. 6

[CDA99] COTIN S., DELINGETTE H., AYACHE N.: Real-time elastic deformations of soft tissues for surgery simulation. *IEEE Transactions on Visualization and Computer Graphics 5*, 1 (1999), 62–73. 3

[CDC10] COMAS O., DURIEZ C., COTIN S.: Shell model for reconstruction and real-time simulation of thin anatomical structures. In *Medical Image Computing and Computer-Assisted Intervention–MICCAI 2010*. Springer, 2010, pp. 371–379. 5

[CDP07] CHOWDHURY M. M., DAGASH H., PIERRO A.: A systematic review of the impact of volume of surgery and specialization on patient outcome. *British Journal of Surgery 94*, 2 (2007), 145–161. URL: http://dx.doi.org/10.1002/bjs.5714, doi:10.1002/bjs.5714. 1

[DAK] DURIEZ C., ANDRIOT C., KHEDDAR A.: Interactive haptics for virtual prototyping of deformable objects: snap-in tasks case. *feedback 20*, 28. 3

[DDKA06] DURIEZ C., DUBOIS F., KHEDDAR A., ANDRIOT C.: Realistic haptic rendering of interacting deformable objects in virtual environments. *IEEE Transactions on Visualization and Computer Graphics 12* (2006), 36–47. 3, 6

[DVWS*11] DE VISSER H., WATSON M. O., SALVADO O., PASSENGER J. D., ET AL.: Progress in virtual reality simulators for surgical training and certification. *Medical Journal of Australia 194*, 4 (2011), S38. 1

[EHA*14] ECHEGARAY G., HERRERA I., AGUINAGA I., BUCHART C., BORRO D.: A brain surgery simulator. *Computer Graphics and Applications, IEEE 34*, 3 (2014), 12–18. 3

[FD15] FENZ W., DIRNBERGER J.: Real-time surgery simulation of intracranial aneurysm clipping with patient-specific geometries and haptic feedback. In *SPIE Medical Imaging* (2015), International Society for Optics and Photonics, pp. 94150H–94150H. 3

[FLA*05] FRANCE L., LENOIR J., ANGELIDIS A., MESEURE P., CANI M.-P., FAURE F., CHAILLOU C.: A layered model of a virtual human intestine for surgery simulation. *Medical image analysis 9*, 2 (2005), 123–132. 3

[FM81] FU K.-S., MUI J.: A survey on image segmentation. *Pattern recognition 13*, 1 (1981), 3–16. 4

[GC04] GALLAGHER A. G., CATES C. U.: Approval of virtual reality training for carotid stenting: what this means for procedural-based medicine. *Jama 292*, 24 (2004), 3024–3026. 1

[GO09] GARRE C., OTADUY M. A.: Haptic rendering of complex deformations through handle-space force linearization. In *World Haptics Conference* (2009), IEEE, pp. 422–427. doi:10.1109/WHC.2009.4810813. 3

[JP05] JAMES D. L., PAI D. K.: A unified treatment of elastostatic contact simulation for real time haptics. In *SIGGRAPH '05: ACM SIGGRAPH 2005 Courses* (2005), p. 141. 3

[LPJ12] L T., P B., JP L.: Surgery for unruptured intracranial aneurysms in the isat and isuia era. *Can J Neurol Sci 39* (2012), 174–179. 1

[MG*02] MOLYNEUX A., GROUP I. S. A. T. I. C., ET AL.: International subarachnoid aneurysm trial (isat) of neurosurgical clipping versus endovascular coiling in 2143 patients with ruptured intracranial aneurysms: a randomised trial. *The Lancet 360*, 9342 (2002), 1267–1274. 1

[MH04] MAHVASH M., HAYWARD V.: High-fidelity haptic synthesis of contact with deformable bodies. *IEEE Comput. Graph. Appl. 24*, 2 (2004), 48–55. 3

[MPH*00] MIGA M., PAULSEN K. D., HOOPES P. J., KENNEDY JR F. E., HARTOV A., ROBERTS D. W., ET AL.: In vivo quantification of a homogeneous brain deformation model for updating preoperative images during surgery. *Biomedical Engineering, IEEE Transactions on 47*, 2 (2000), 266–273. 3, 5

[PDC11] PETERLIK I., DURIEZ C., COTIN S.: Asynchronous haptic simulation of contacting deformable objects with variable stiffness. In *Intelligent Robots and Systems (IROS), 2011 IEEE/RSJ International Conference on* (France, 2011), pp. 2608–2613. URL: https://hal.archives-ouvertes.fr/hal-00823762. 6

[PL99] PICINBONO G., LOMBARDO J.-C.: Extrapolation: a solution for force feedback? In *International Scientific Workshop on Virtual Reality and Prototyping* (Laval France, June 3-4 1999), pp. 117–125. 3

[PMRA09] PAOLIS L. T. D., MAURO A. D., RACZKOWSKY J., ALOISIO G.: Virtual model of the human brain for neurosurgical simulation. *Studies in health technology and informatics* (2009), 811–815. 3

[PND*11] PETERLIK I., NOUICER M., DURIEZ C., COTIN S., KHEDDAR A.: Constraint-based haptic rendering of multirate compliant mechanisms. *IEEE Trans. Haptics 4*, 3 (2011), 175–187. 3

[PSBM10] PETERLIK I., SEDEF M., BASDOGAN C., MATYSKA L.: Real-time visio-haptic interaction with static soft tissue models having geometric and material nonlinearity. *Computers & Graphics 34*, 1 (2010), 43–54. 3

[WoUIAI*03] WIEBERS D. O., OF UNRUPTURED INTRACRANIAL ANEURYSMS INVESTIGATORS I. S., ET AL.: Unruptured intracranial aneurysms: natural history, clinical outcome, and risks of surgical and endovascular treatment. *The Lancet 362*, 9378 (2003), 103–110. 1

[ZC99] ZHUANG Y., CANNY. J.: Real-time simulation of physically realistic global deformation. In *"Hot-topic", in IEEE Visualization Conference* (San Francisco, 1999). 3